Journal of Molecular Catalysis B: Enzymatic 62 (2010) 190–196

Contents lists available at ScienceDirect

Journal of Molecular Catalysis B: Enzymatic

journal homepage: www.elsevier.com/locate/molcatb

Conjugation of nattokinase and lumbrukinase with magnetic nanoparticles for the assay of their thrombolytic activities

Lili Ren[a], Xuming Wang[a], Heng Wu[a], Bingbing Shang[a], Jinyi Wang[a,b,c,*]

[a] College of Life Science and College of Science, Northwest A&F University, Yangling, Shaanxi 712100, PR China
[b] College of Veterinary Medicine, Northwest A&F University, Yangling, Shaanxi 712100, PR China
[c] Shaanxi Key Laboratory of Molecular Biology for Agriculture, Northwest A&F University, Yangling, Shaanxi 712100, PR China

ARTICLE INFO

Article history:
Received 1 July 2009
Received in revised form 14 October 2009
Accepted 27 October 2009
Available online 31 October 2009

Keywords:
Nattokinase
Lumbrukinase
Magnetic nanoparticle
Conjugate
Thrombolysis

ABSTRACT

Two important thrombolytic enzymes, nattokinase (NK) and lumbrukinase (LK), were immobilized onto fine magnetic Fe_3O_4 nanoparticles using 1-[3-(dimethylamino)propyl]-3-ethylcarbodiimide (EDC) as the coupling reagent, and their thrombolytic activities were studied. The Fe_3O_4 nanoparticles and NK- and LK-conjugated magnetic nanoparticles were characterized by transmission electron microscopy, Fourier transform infrared spectrophotometry, vibrating sample magnetometry, X-ray diffraction, and UV–vis absorption spectroscopy. Dual kinetic absorbance measurements at 405 and 630 nm were employed to measure their thrombolytic activity. Analysis of protein amount showed that the optimum conditions for NK and LK binding to nanoparticles were respectively at a mass ratio of 2:1:1, 2:1:2 (magnetic nanoparticles:protein:EDC), and pH 6.00. Thrombolytic activity assay showed that the best thrombolytic activity could reach 91.89% for NK–nanoparticle conjugates and 207.74% for LK–nanoparticle conjugates, which are much higher than the pure enzymes (NK, 82.86%; LK, 106.57%).

1. Introduction

Thrombotic events affect many individuals in a number of ways, all of which can cause significant morbidity and mortality [1–5]. According to the report of the World Health Organization, 17 million people die of cardiovascular diseases every year [6]. Previous studies demonstrated that intravascular thrombosis, a blood clot in a blood vessel, is one of the main causes for various thrombotic events, and the major component of blood clots is fibrin formed from fibrinogen during the proteolysis by thrombin [3,7–10]. Meanwhile, fibrin clots can be hydrolyzed by plasmin to avoid thrombosis in blood vessels. In a normal situation, these reactions are kept at a balance. However, once the balanced situation is triggered by some disorders, the clots cannot be hydrolyzed, and thus thrombosis occurs [11]. Based on the working mechanisms, two kinds of thrombolytic agents have been developed and been applied in clinic therapy [4–6,12]: (1) plasminogen activator, such as tissue-type plasminogen activator (t-PA), streptokinase, and urokinase, which activate plasminogen into active plasmin to degrade fibrin; and (2) plasmin-like proteins, such as nattokinase, lumbrukinase, and fibrolase, which directly degrade the fibrin in blood clots.

Of the thrombolytic enzymes mentioned above, nattokinase was reported to not only possess plasminogen activator activity, but also directly digests fibrin through limited proteolysis. Its fibrinolytic activity can be retained in the blood for more than 3 h. It was also reported that nattokinase is less sensitive to the cleavage of fibrinogen, but is more sensitive to the cleavage of cross-linked fibrin compared to plasmin [6,13–17]. Earthworm fibrinolytic enzymes (lumbrukinase) are a group of serine proteases that have strong fibrinolytic and thrombolytic activities [2,18,19]. Therefore, these two enzymes have been regarded as promising agents for thrombosis therapy. However, plasmin in blood has a short half-life, and its expensive price and undesirable side-effects prompt researchers to search for cheaper and safer resources [6]. In addition, all available thrombolytic agents suffer significant shortcomings, including large therapeutic doses, limited efficacy, reocclusion, and bleeding complications, thus discouraging their widespread application [1,5,7,20].

To address these problems and improve therapy effectivity, targeting the delivery of these thrombolytic agents to localized diseases has gained increasing interest over the past decade in the field of nanobiotechnology [21–24]. Among them, magnetite (Fe_3O_4) nanoparticles were found to have extensive applications in this field since the 1960s due to their magnetic and electronic properties [25–29], good biocompatibility, low toxicity, and easy drug-binding characteristics by changing their surface properties [30]. To date, the targeting of drug-bearing magnetic particles to a specific part of the body has been studied using magnetic flu-

* Corresponding author at: College of Science, No. 3 Taicheng Rd., Northwest A&F University, Yangling, Shaanxi 712100, PR China. Tel.: +86 29 87082520; fax: +86 29 87082520.
E-mail address: jywang@nwsuaf.edu.cn (J. Wang).

1381-1177/$ – see front matter © 2009 Elsevier B.V. All rights reserved.
doi:10.1016/j.molcatb.2009.10.009

ids, unstable suspensions, and magnetic microspheres [31,32]. All of these demonstrate that Fe_3O_4 nanoparticles are ideal for carrying small molecular weight pharmacologically active substances to a target area. In addition, the resulting enzymes conjugated on the magnetic particles have long-term stability and high enzymatic activity [33–35].

In earlier studies, an attempt was made to link streptokinase, a thrombolytic agent, directly to magnetic particles using 1-[3-(dimethylamino)propyl]-3-ethylcarbodiimide (EDC) as the coupling agent. The immobilized streptokinase was assayed *in vitro* by lysing the standard fibrin clot. The magnetic properties of the particle–streptokinase congener allow the treatment to be focused to the exact location where the clot was located, thus reducing the amount of enzyme required and, in turn, reducing the risk of eliciting an immune response [24,28]. However, the dynamic process of the formation and lysis of clots have not yet been studied. In particular, the action of nattokinase and lumbrukinase has not been reported to date according to our best knowledge.

In the present study, an attempt was made to link the protein molecules NK and LK directly to magnetic particles using EDC as the coupling agent. Different values of pH and mass ratios of magnetic particles (MNPs) to protein and to EDC were studied in order to establish the optimum conditions for immobilization. Meanwhile, systemic assay of the coagulation and thrombolytic capacities was further investigated, which not only showed the whole process of thrombosis, but also the process of thrombolysis under different conditions.

2. Materials and methods

2.1. Materials

The fibrinogen and thrombin used in this work were obtained from Sigma–Aldrich (St. Louis, MO). The BCA™ Protein Assay Kit was purchased from Pierce Biotechnology (Rockford, IL). The NK (20,000 FU/mg) was obtained from Tianyi Biotech, Ltd. (Xi'an, China), while the LK (16,000 U/mg) was received from Guoyuan Biotech, Ltd. (Shanghai, China). The 1-[3-(dimethylamino)propyl]-3-ethylcarbodiimide (EDC) was purchased from GL Biochem, Ltd. (Shanghai, China). All solvents and other chemicals were purchased from local commercial suppliers and were of analytical reagent grade, unless otherwise stated. All solutions were prepared using distilled and deionized water.

2.2. Preparation of magnetic Fe_3O_4 nanoparticles

Magnetic Fe_3O_4 nanoparticles were prepared by coprecipitating ferric and ferrous salts in an alkaline solution [25,26,35]. 3 mL $FeCl_3$ (2 M dissolved in 2 M HCl) was first added to 10.33 mL double distilled water, and 2 mL Na_2SO_3 (1 M) was then added dropwisely within 1 min under magnetic stirring. Just after mixing the solutions, the color of the solution changed from light yellow to red, indicating complex ions formed between the Fe^{3+} and SO_3^{2-}. When the solution returned to its original color, 80 mL $NH_3{\cdot}H_2O$ solution (0.85 M) was added under vigorous stirring. A black precipitate quickly formed, which was allowed to crystallize completely for another 30 min under magnetic stirring. The precipitate was washed with deoxygenated water by magnetic decantation until the pH value of the suspension was less than 7.5. After sealing, the prepared Fe_3O_4 was stored in a refrigerator prior to use.

2.3. Conjugation of NK and LK onto magnetic Fe_3O_4 nanoparticles

The conjugation of NK and LK onto magnetic particles was performed using a protocol reported previously [28]. To determine the optimum conditions for NK and LK immobilization, also, the coupling reactions were carried out under different conditions, including the pH value of the reaction mixture and the proportion of magnetic nanoparticles (MNPs) to protein to EDC (MNPs:protein:EDC). All steps were performed at room temperature and in a laminar flow hood to maintain sterility of all reagents. Caution was used in handling biological materials.

For a given value of pH 5.14 and a mass ratio of 2:1:2 (MNPs:NK:EDC), 0.5 mL of NK solution (20 mg/mL, pH 5.14 in 0.003 M sodium and potassium phosphate buffer) was added into 1 mL of EDC solution (20 mg/mL dissolved in the same buffer). Then, 1 mL of magnetic particles (20 mg/mL in the same buffer, pH 5.14) was added to the mixture. After shaking for 24 h in a shaker incubator, the protein-conjugated nanoparticles were separated with a magnet, and were stored in a refrigerator at 4 °C until use. All of the other experiments for coupling condition optimization were also performed following the same procedures described above.

2.4. Analysis of the amount of protein drugs bound onto the nanoparticles

To analyze the amount of protein drugs (NK and LK) bound onto the magnetic nanoparticles, the concentrations of each protein drug in the initial solutions and in the reaction supernatants after immobilization were determined with the BCA™ Protein Assay Reagent Kit using a microplate reader (Bio-Rad Model 680, USA). The amount of protein drug attached onto the magnetic nanoparticles was then calculated as

$$D = \frac{C_i V_i - C_f V_f}{W}$$

where D is the amount of protein drug (NK or LK) bound onto magnetic nanoparticles (mg/mg), C_i and C_f are the concentrations of the initial and final protein drug in the reaction medium (mg/mL), respectively, and V_i and V_f are the volumes of the reaction medium (mL). Herein, W is the weight of the magnetic nanoparticles (mg).

2.5. Characterization methods

The size of Fe_3O_4 nanoparticles and protein-conjugated nanoparticles were characterized by transmission electron microscopy (TEM, JEM-3010, with EDS of Oxford INCA and CCD Camera of Gatan 894, Japan). The crystal structure was characterized by an X-ray diffractometer (XRD, Philips D/Max-2500, Holland) using a monochromatized X-ray beam with nickel-filtered Cu Kα radiation. Magnetic measurements of Fe_3O_4 nanoparticles and protein-conjugated nanoparticles were carried out on a vibrating sample magnetometer (VSM, LAKESHORE-7304, USA) by changing H between +4000 and −4000 Oe. The FT-IR spectra of protein-conjugated nanoparticles were recorded using Fourier transform infrared spectroscopy (Nicolet NEXUS 670, USA).

2.6. Activity measurement

For each drug protein-conjugated nanoparticle sample analyzed for thrombolytic activity, 100 μL of fibrinogen (3 mg/mL) was added into two wells of 96-well Elisa plates (Jet Biofil). After warmed for 3 min at 37 °C, 0.72 μL of thrombin (140 units/mL) was mixed in each of the two wells. Then, the plate was immediately placed in an eight-channel microplate reader (Bio-Rad 680) for dual kinetic absorbance measurements at 405 and 630 nm. Data were recorded continuously at a 60 s interval for 2 h. After that, 100 μL of pure NK or LK and particle–NK or –LK congener solutions (0.2 mg/mL) were added into the mixture, respectively. Followed by 1 s mixing step, the absorbance of the reaction mixtures were then continuously recorded for another 2 h under the same conditions. Each experiment was repeated three times. Blank controls were

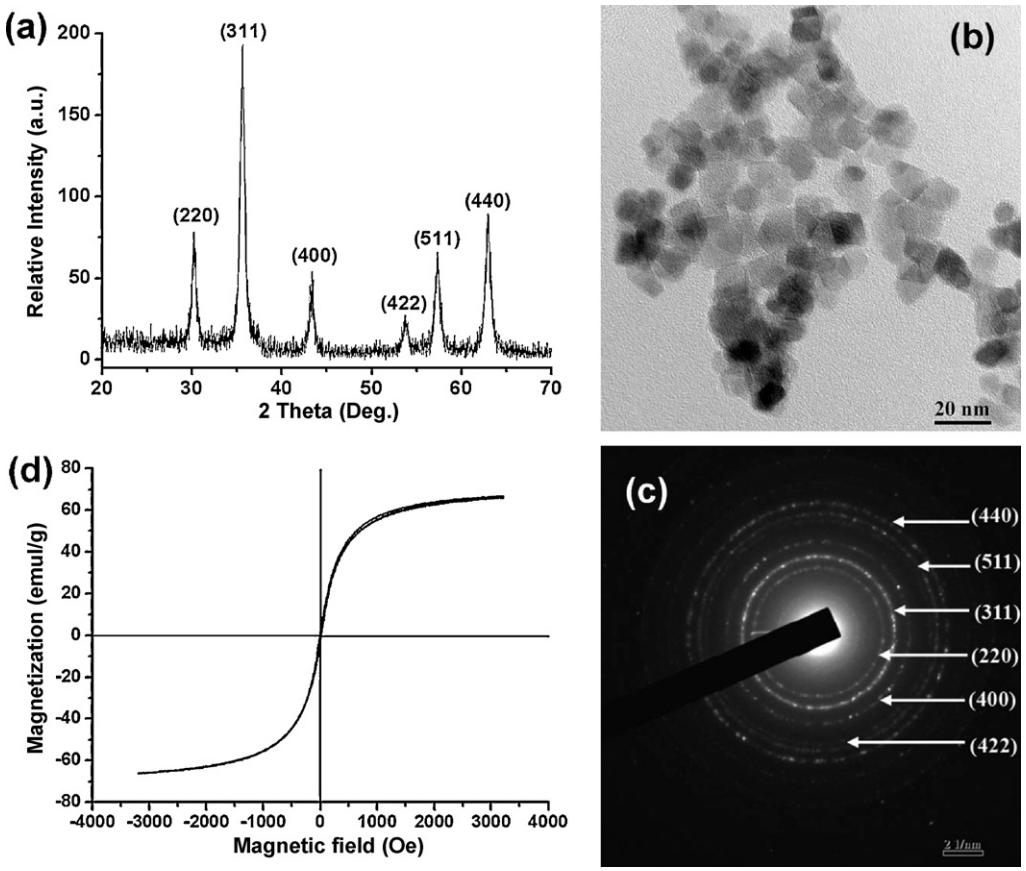

Fig. 1. (a) XRD pattern of the prepared Fe_3O_4 nanoparticles. (b) TEM image of the prepared Fe_3O_4 nanoparticles. Scale bar = 20 nm. (c) ED pattern of the prepared Fe_3O_4 nanoparticles. Scale bar = 21 nm. (d) The magnetization curves of the prepared Fe_3O_4 nanoparticles (Hc = 12.5 Oe; Ms = 66 emu/g; Hs = 1500 Oe).

run concomitantly during each experiment using 200 μL of physiological saline [36]. Thrombolytic activity was then calculated as follows:

$$F_a = \frac{A_m - A_f}{A_m - A_i} \times 100 \quad (1)$$

where F_a is the thrombolytic activity of the analyzed sample, A_m is the maximum absorbance, and A_i and A_f are the initial baseline absorbance and the final absorbance of the reaction mixture, respectively.

To investigate the inhibitory ability of the two enzymes and their particle congeners during the blood clot formation, their inhibitory ability were also investigated by adding pure NK or LK, respectively. Their particle congeners were likewise included into the mixture of fibrinogen and thrombin, both of which were present, at the beginning of each experiment. The experimental procedure was the same as described above. The inhibitory range of each sample was then calculated as follows:

$$I_r = A_f - A_i \quad (2)$$

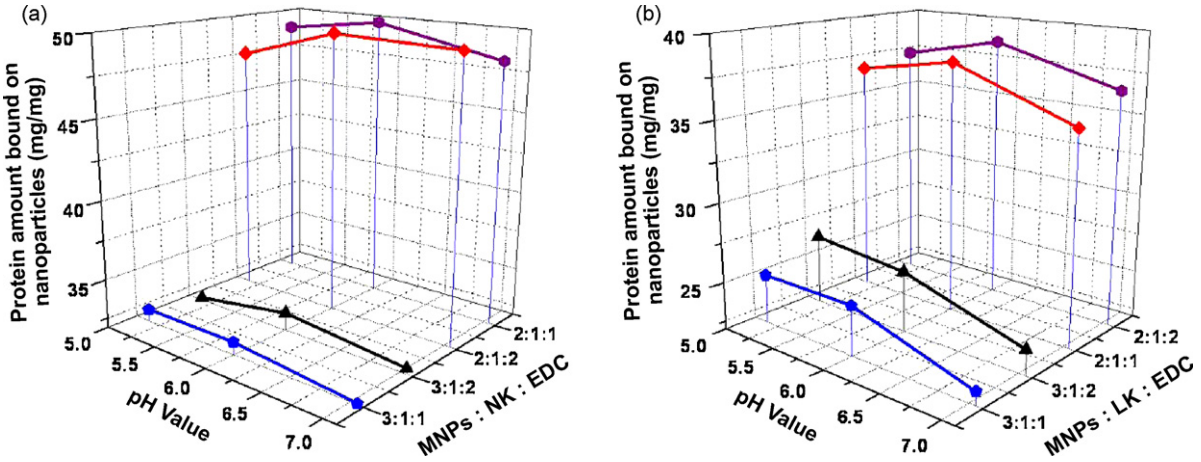

Fig. 2. Effect of coupling reaction conditions on the protein drug amount bound on Fe_3O_4 nanoparticles. (a) Effect of pH value of the coupling reaction medium and the ratio of MNPs:NK:EDC on protein NK amount bound on Fe_3O_4 nanoparticles. (b) Effect of pH value of the coupling reaction medium and the ratio of MNPs:LK:EDC on protein LK amount bound on Fe_3O_4 nanoparticles.

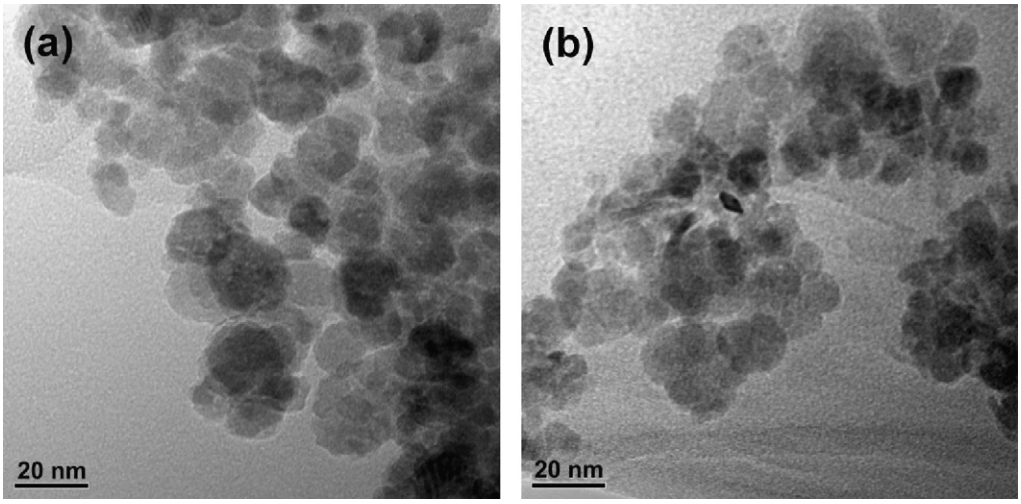

Fig. 3. TEM images of NK–Fe_3O_4 nanoparticle conjugates (a) and LK–Fe_3O_4 nanoparticle conjugates (b). Scale bar = 20 nm.

where I_r is the inhibitory range of each sample, A_m is the maximum absorbance, and A_i and A_f are the initial baseline absorbance and the final absorbance, respectively.

3. Results and discussion

3.1. Synthesis and characterization of Fe_3O_4 nanoparticles

The Fe_3O_4 nanoparticles were used as the magnetic carrier in this study, and were synthesized by a chemical coprecipitation of Fe^{2+} and Fe^{3+} ions under alkaline condition [25,27,35]. The X-ray powder diffraction (XRD) pattern of the as-prepared product shown in Fig. 1(a) confirms its crystalline nature and also verifies the peaks that were well matched with standard Fe_3O_4 reflections. The presented XRD pattern featured six strong Bragg diffraction peaks at 20–70° 2θ (2θ = 30.08, 35.42, 43.08, 53.56, 56.98, and 62.62), which can be indexed as (2 2 0), (3 1 1), (4 0 0), (4 2 2), (5 1 1), and (4 4 0). The results confirmed the successful synthesis of Fe_3O_4 using a cubic spinel structure (JCPDS card no. 85-1436).

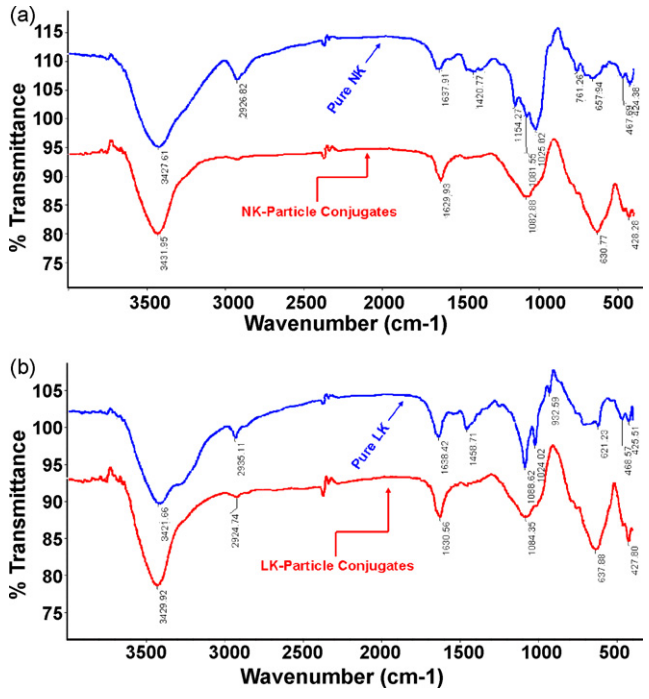

Fig. 4. (a) FT-IR spectra of pure NK protein (top) and NK–Fe_3O_4 nanoparticle conjugates (bottom); (b) FT-IR spectra of pure LK protein (top) and LK–Fe_3O_4 nanoparticle conjugates (bottom).

Fig. 1(b) shows a TEM image of the Fe_3O_4 nanoparticles, indicating that nanosized Fe_3O_4 particles of uniform morphology and good dispersion had been generated. The diameter of a single Fe_3O_4 nanoparticle was estimated to be in the range of 8–15 nm. Electron diffraction (ED) patterns (Fig. 1(c)) which correspond to bright field images show that these particles consisted of Fe_3O_4 nanoparticles with a cubic spinel structure. This again provides supportive evidence that Fe_3O_4 nanoparticles had been created.

Fig. 1(d) shows the magnetization curve of the prepared Fe_3O_4 nanoparticles, which demonstrates a symmetrical hysteresis loop. This phenomenon is characteristic of a material that is superparamagnetic in nature; in other words, the Fe_3O_4 nanoparticles can become magnetized in the presence of a magnetic field. Once the field is taken away from the particles, only a minimal residual magnetization remains within the particles. This makes these particles ideal for further magnetic targeted therapy, as the nanoparticles might be taken to the located clots in the body via the action of an external magnetic field [29,32,34,35]. The saturation magnetization (Ms) and coercivity (Hc) of the Fe_3O_4 nanoparticles were 66 emu/g and 12.5 Oe.

3.2. Preparation and characterization of NK- and LK-conjugated magnetic nanoparticles

3.2.1. Preparation of NK- and LK-conjugated magnetic nanoparticles

In the current study, the magnetic particles are synthesized by the coprecipitation method resulting in the formation of macroions [25,27,35]. The specific adsorption of the amphoteric hydroxyl (–OH) group imparts both superficial negative charges to the particles in an alkaline medium and positive charges in an acidic medium. Bacri et al. [37] have shown that the –OH ligand will remain on the particles at a pH between 6 and 10. Thus, in the present case, the free hydroxyl group on the surface of the particles is responsible for the binding of the protein. First, the 1-[3-(dimethylamino)propyl]-3-ethylcarbodiimide hydrochloride (EDC) modifies the carboxyl group of the protein at a slightly acidic pH [38], then the proteins become conjugated onto magnetic nanoparticles by an ester bond. However, the protein analysis by BCA protein protocol showed that different conditions could directly influence the amount of drug protein bound onto the

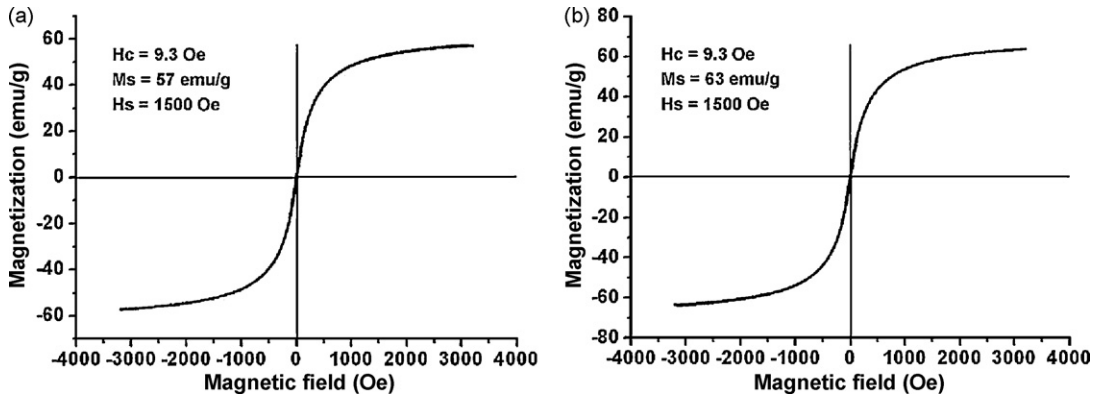

Fig. 5. The magnetization curves of NK–Fe_3O_4 nanoparticle conjugates (a, Ms = 57 emu/g, Hc = 9.3 Oe, and Hs = 1500 Oe) and LK–Fe_3O_4 nanoparticle conjugates (b, Ms = 63 emu/g, Hc = 9.3 Oe, and Hs = 1500 Oe).

nanoparticles. To determine optimum conditions for conjugation, the pH value of the reaction mixture and the proportion of magnetic nanoparticles (MNPs) to protein to EDC (MNPs:protein:EDC) were also optimized in this study. The results are shown in Fig. 2.

Fig. 2 shows the optimum condition for binding NK onto magnetic nanoparticles at a mass ratio of 2:1:1 (MNPs:NK:EDC) and pH 6.00. The optimum conditions for higher amount binding of LK onto the magnetic particles were observed at a mass ratio of 2:1:2 (MNPs:LK:EDC) and pH 6.00. The optimum amount of protein drug bound onto the nanoparticles was 49.89% (w/w) for NK and 38.74% (w/w) for LK.

3.2.2. *Characterization of NK- and LK-conjugated magnetic nanoparticles*

Fig. 3 illustrates the TEM images of NK- and LK-conjugated magnetic nanoparticles, which show that proteins are layered over the magnetic particles with an average diameter of 12–24 nm for NK and 12–20 nm for LK. Fig. 4(a) shows the FT-IR spectral characteristics of NK bound to the magnetic particles. It was evident that the characteristic bands of protein NK at 3430, 1630, and 1000 cm^{-1} are present in pure NK and NK-bound magnetic nanoparticles. The Fe–O band was also observed at 630 cm^{-1}. Fig. 4(b) shows the FT-IR spectra of pure LK and LK-bound magnetic particles, which also indicates similar results. The characteristic bands of protein LK at 3420, 1630, and 1080 cm^{-1} were present in pure LK and LK-conjugated magnetic nanoparticles, and the characteristic band of Fe–O was also observed at 637 cm^{-1}. Overall, the FT-IR spectra also provide supportive evidence that the NK and LK proteins had been conjugated onto the magnetic nanoparticles.

A study of the magnetic performance of the protein-bound magnetic nanoparticles using a vibrating sample magnetometer (VSM) shows that their magnetization curves (Fig. 5) were also in a symmetrical hysteresis loop, with an Ms of 57 emu/g for NK-conjugated magnetic nanoparticles and 63 emu/g for LK-conjugated particles. Their coercivity was 9.3 Oe for NK-conjugated nanoparticles and 9.3 Oe for LK-conjugated nanoparticles. This phenomenon indicates that the prepared Fe_3O_4–protein nanoparticles are also superparamagnetic [24,33]. Compared with the Fe_3O_4 nanoparticles, the protein-bound nanoparticles exhibited a relatively low Ms. This may have been a result of protein binding onto the particle surface, which may then quench the magnetic moment [33].

To further ascertain if the protein-bound nanoparticles in the aqueous phase have good response to an external magnetic field, the magnetic performance of protein-bound nanoparticles in a physiological saline was also studied using an external magnetic field and a UV–vis spectrophotometer (Mapada UV-1600PC, Shanghai). Fig. 6 shows the magnetic separation property of the protein microspheres, which was determined through the transmittance of the microsphere suspension after being separated by a 0.42 T magnetic field for a certain time. Experimental results show that magnetic separation of protein-bound nanoparticles is rapid and easy. Also, they still retained satisfactory magnetic-responsive aggregation and redispersion properties (Fig. 6, inserts). Transmittance of magnetic separation suspension neared 98.3% for NK-conjugated nanoparticles and 96.6% for LK-conjugated particles within 1 h, whereas separation by deposition in the gravity state required at least 4 h to reach 72.1% transmittance for NK-conjugated particles and 66.4% transmittance for LK-conjugated particles. All of these results indicate that these protein-bound particles also possess excellent magnetic performance in aqueous phase.

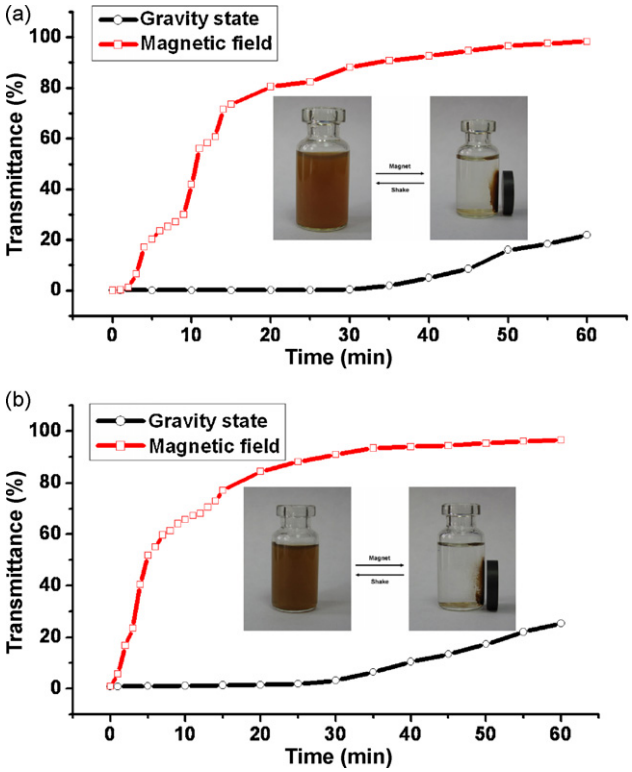

Fig. 6. The magnetic separation property of protein drug–nanoparticle conjugate suspension in a magnetic field and under gravity (a, NK–Fe_3O_4 nanoparticle conjugates in physiological saline; b, LK–Fe_3O_4 nanoparticle conjugates in physiological saline). Inserts in (a) and (b) are the protein drug (NK or LK) in physiological saline and their response to an external magnetic field.

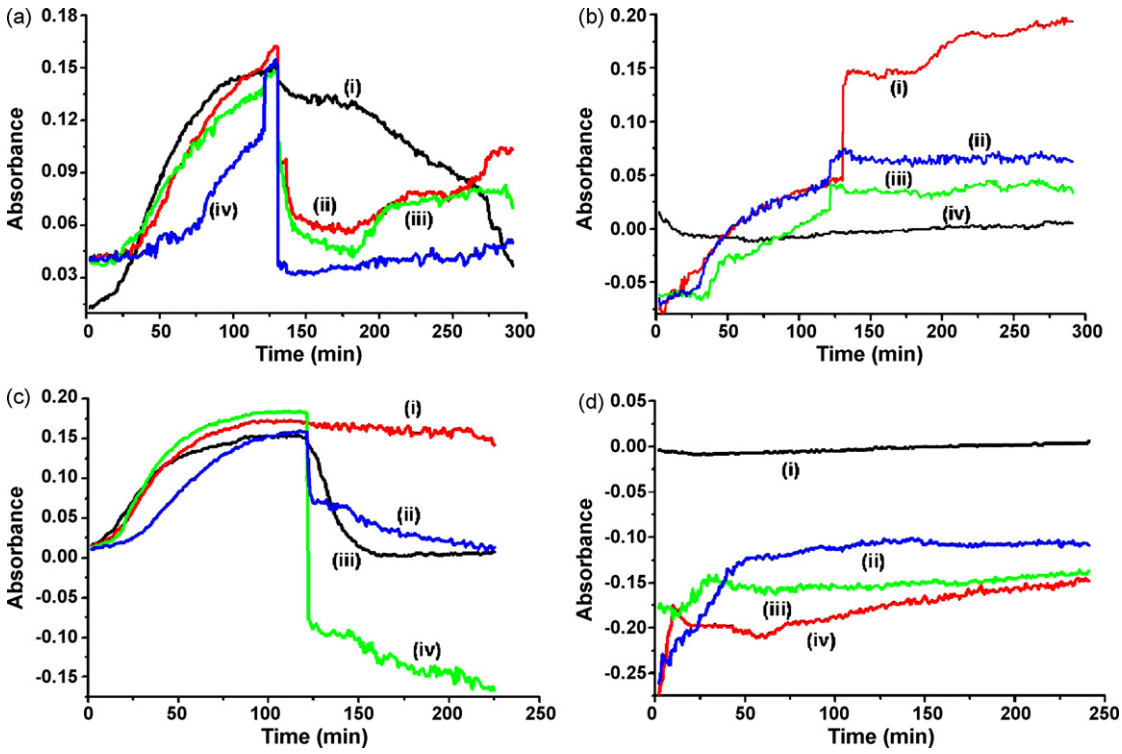

Fig. 7. Thrombolytic and inhibitory activity analysis of pure protein drug and protein drug–nanoparticle conjugates. (a) Temporal changes of absorbance of the reaction mixture of fibrinogen and thrombin before and after the addition of different protein NK drugs (i, pure NK; ii–iv, NK–Fe_3O_4 nanoparticle conjugates prepared at pH 5.14, 6.00, 7.05, and a corresponding mass ratio of 2:1:1, 2:1:1, and 2:1:2 (MNPs:NK:EDC), respectively). (b) Temporal changes of absorbance of the reaction mixture of fibrinogen and thrombin before and after the addition of different protein LK drugs (i, ii and iv, LK–Fe_3O_4 nanoparticle conjugates prepared at pH 5.14, 7.05, 6.00, and a corresponding mass ratio of 2:1:2, 2:1:2, and 2:1:2 (MNPs:LK:EDC), respectively; iii, pure LK). (c) Temporal changes of absorbance of the reaction mixture of fibrinogen, thrombin, and different protein NK drugs (i–iii, NK–Fe_3O_4 nanoparticle conjugates prepared at pH 5.14, 7.05, 6.00, and a corresponding mass ratio of 2:1:1, 2:1:2, and 2:1:1 (MNPs:NK:EDC), respectively; iv, pure NK). (d) Temporal changes of absorbance of the reaction mixture of fibrinogen, thrombin, and different protein LK drugs (i, pure LK; ii–iv, LK–Fe_3O_4 nanoparticle conjugates prepared at pH 7.05, 6.00, 5.14, and a corresponding mass ratio of 2:1:2, 2:1:2, and 2:1:2 (MNPs:LK:EDC), respectively).

3.3. Activity measurement

In our preliminary study, we found that blood clots produced by fibrinogen and thrombin differed at varying ratios of fibrinogen to thrombin. In order to facilitate the *in vitro* study, conditions for the formation of blood clots were optimized in our laboratory prior to activity measurement [4,11,39–41]. The optimum conditions for the final concentrations of fibrinogen and thrombin used were 3 mg/mL and 0.001 units/μL, which allowed for relatively high stability and suited rate of formation of clots.

Based on the optimized concentration of fibrinogen and thrombin, the thrombolytic activity and inhibitory activity of the protein-bound particles, as well as the pure NK and LK, were all considered in the current study. Additionally, to further investigate the influence of the pH value of the coupling reaction medium on the activity of protein drugs, two other protein-bound particles prepared at different pH values were also studied for NK and LK, respectively. The results are shown in Fig. 7.

From Fig. 7(a) and (b) we can clearly see that the addition of thrombin to the fibrinogen solution achieves activated blood coagulation, resulting in fibrin clot formation associated with increased optical density. When pure proteins and protein–particle conjugates were added, fibrinolysis process was initiated, exhibiting a relative decrease of optical density (which we can clearly see before and after the Inflexion of a Curve). All of these results imply that the change of absorbance on the curve represents the thrombi level, and gives general information about fibrin generation and lysis throughout the measurement [8]. From the results, we can also see that the curves reflect the dynamic contributions of ongoing coagulation activation and fibrinolysis reactions during the course of clot formation and lysis.

Although a dynamic interaction between coagulation activation and fibrinolysis likely proceeds throughout the entire course of this assay, the former appears to contribute most to the phase of rise in absorbance. Similarly, fibrinolysis appears to contribute most to the decline phase in absorbance. The biochemical processes of the decline in absorbance are not yet completely understood; however, it is possible that the lysis phase represents fibrin reorganization during fibrinolysis and later, fibrin dissolution [36].

In the study of the inhibitory ability of the pure protein and protein–particle conjugates, we also find that they all show excellent inhibitory ability (Fig. 7(c) and (d)). The thrombolytic and inhibitory activities are listed in Tables 1 and 2, respectively. From the results, we find that the NK-conjugated nanoparticles prepared at pH 7.05 (MNPs:protein:EDC = 2:1:2) offered the best throm-

Table 1
Thrombolytic and inhibitory activities of pure protein NK and NK–Fe_3O_4 nanoparticle conjugates prepared at different pH values of the coupling reaction medium.

NK or immobilized NK on MNPs at various pH values	Activity of NK	
	Thrombolytic activity (%)	Inhibitory range
pH 5.14[a]	48.76	0.268
pH 6.00[a]	71.96	0.095
pH 7.05[b]	91.89	0.128
Pure NK	82.86	−0.011

[a] Mass ratio = 2:1:1 (MNPs:NK:EDC).
[b] Mass ratio = 2:1:2 (MNPs:NK:EDC).

Table 2
Thrombolytic and inhibitory activities of pure protein LK and LK–Fe_3O_4 nanoparticle conjugates prepared at different pH values of the coupling reaction medium.

LK or immobilized LK on MNPs at various pH values	Activity of LK	
	Thrombolytic activity (%)	Inhibitory range
pH 5.14[a]	18.06	0.126
pH 6.00[a]	207.74	0.04
pH 7.05[a]	97.97	0.152
Pure LK	106.57	0.01

[a] Mass ratio = 2:1:2 (MNPs:LK:EDC).

bolytic activity (91.89%), even higher than the pure NK (82.86%). The possible reasons may be that immobilization of enzyme on the magnetic particles can protect them from denaturation and self-digestion, resulting in their long-term stability and high enzymatic activity. Additionally, immobilization concentrates enzyme on the particles and therefore accelerates the speed of their action [33,42]. Meanwhile, thrombolytic activity increased with the increasing pH value used when preparing the protein–particle conjugates. One possible reason may be that the basic condition can activate the NK's activity, which was in agreement to the results from the study of NK's fibrinogenolysis and fibrinolysis at different pH values in our laboratory. However, the inhibitory range is slightly different, corresponding to the amount of protein bound onto the nanoparticles; that is, the higher the drug amount, the higher the inhibitory activity. Compared with the pure NK, protein drug-conjugated particles possessed low inhibitory activity. One possible reason may be that the protein–particles were not homogeneous in the reaction medium.

For pure LK and LK-particle conjugates, the results, as shown in Fig. 7(b) and (d) and Table 2, indicate that the LK-particle conjugates prepared at pH 6.00 (MNPs:protein:EDC = 2:1:2, corresponding to the highest protein-bound amount) offered the best thrombolytic activity (207.74%), which was much higher than that of pure LK (106.57%). Their inhibitory ranges also manifest the same trend with the protein-bound amount.

In comparison, the thrombolytic activity of pure LK is apparently higher than that of pure NK, but a bit weaker in terms of inhibitory activity. According to the protein–particle conjugates with the highest protein-bound amount, the immobilized LK has stronger activity than immobilized NK both in thrombolytic and inhibitory activities, even stronger than those of pure NK and LK. All of these results indicate that both NK and LK have fibrinogenolysis and fibrinolysis. They can be used as anticoagulants and thrombolysis agents. Moreover, based on the results, it is known that using the enzymes at the initial stage of thrombosis can effectively inhibit the formation of thrombi.

4. Conclusions

In summary, NK and LK were first well immobilized onto magnetic nanoparticles in the presence of EDC without the aid of a primary coating. The activity assay showed that they all had good thrombolysis and inhibition of thrombosis, even higher than the pure NK and LK. As such, they can be used as promising thrombolytic agents to benefit people suffering from thrombotic diseases. Furthermore, the preparation method of magnetic nanoparticles immobilized with thrombolytic enzymes and evaluation method of thrombolytic activity can be directly and conveniently applied in daily studies of thrombolytic drugs and diseases. However, improvements and related research remain necessary for it to become more effective and practical to clinical use for thrombolytic events.

Acknowledgments

The authors would like to acknowledge funding from the National Natural Science Foundation of China (no. 207 750 59; no. 209 750 82), the Ministry of Education of the People's Republic of China (NCET-08-0464), and the Northwest A&F University.

References

[1] N. Mackman, Nature 451 (2008) 914–918.
[2] H. Ji, L. Wang, H. Bi, L. Sun, B. Cai, Y. Wang, J. Zhao, Z. Du, Eur. J. Pharmacol. 590 (2008) 281–289.
[3] J.F. Viles-Gonzalez, V. Fuster, J.J. Badimon, Am. Heart J. 149 (2005) 519–531.
[4] H. Li, Z. Hu, J. Yuan, H. Fan, W. Chen, S. Wang, S. Zheng, Z. Zheng, G. Zou, Phytother. Res. 21 (2007) 1234–1241.
[5] D. Collen, H.R. Lijnen, Fibrinolysis Proteol. 14 (2000) 66–72.
[6] Y. Peng, X. Yang, Y. Zhang, Appl. Microbiol. Biotechnol. 69 (2005) 126–132.
[7] G.C. White II, Thromb. Res. 122 (2008) S1–S2.
[8] S. He, A. Antovic, M. Blombäck, Thromb. Res. 103 (2001) 355–361.
[9] F. Khan, L.M. Snyder, L. Pechet, J. Thromb. Thrombolysis 5 (1998) 83–88.
[10] K.F. Standeven, R.A.S. Ariëns, P.J. Grant, Blood Rev. 19 (2005) 275–288.
[11] E.J. Dunn, H. Philippou, R.A.S. Ariëns, P.J. Grant, Diabetologia 49 (2006) 1071–1080.
[12] E.G.R. Fernandes, A.A.A. de Queiroz, G.A. Abraham, J.S. Román, J. Mater. Sci. Mater. Med. 17 (2006) 105–111.
[13] J.G. Liu, J.M. Xing, R. Shen, C.L. Yang, H.Z. Liu, Biochem. Eng. J. 21 (2004) 273–278.
[14] M. Fujita, Y. Ito, K. Hong, S. Nishimuro, Fibrinolysis 9 (1995) 157–164.
[15] R.H. Zhang, L. Xiao, Y. Peng, H.Y. Wang, F. Bai, Y.Z. Zhang, Lett. Appl. Microbiol. 41 (2005) 190–195.
[16] J. Liu, J. Xing, T. Chang, Z. Ma, H. Liu, Process Biochem. 40 (2005) 2757–2762.
[17] Y. Inatsu, N. Nakamura, Y. Yuriko, T. Fushimi, L. Watanasiritum, S. Kawamoto, Lett. Appl. Microbiol. 43 (2006) 237–242.
[18] F. Wang, C. Wang, M. Li, L. Gui, J. Zhang, W. Chang, Biotech. Lett. 25 (2003) 1105–1109.
[19] Y.D. Park, J.W. Kim, B.G. Min, J.W. Seo, J.M. Jeong, Biotech. Lett. 20 (1998) 169–172.
[20] R.A.G. Smith, R.J. Dupe, P.D. English, J. Green, Nature 290 (1981) 505–508.
[21] F.X. Gu, R. Karnik, A.Z. Wang, F. Alexis, E. Levy-Nissenbaum, S. Hong, R.S. Langer, O.C. Farokhzad, Nanotoday 3 (2007) 14–21.
[22] O.C. Farokhzad, J. Cheng, B.A. Teply, I. Sherifi, S. Jon, P.W. Kantoff, J.P. Richie, R. Langer, Proc. Natl. Acad. Sci. U.S.A. 103 (2006) 6315–6320.
[23] A.S. Lübbe, C. Bergemann, J. Brock, D.G. McClure, J. Magn. Magn. Mater. 194 (1999) 149–155.
[24] A.K. Johnson, A.M. Zawadzka, L.A. Deobald, R.L. Crawford, A.J. Paszczynski, J. Nanopart. Res. 10 (2008) 1009–1025.
[25] Y.K. Sun, M. Ma, Y. Zhang, N. Gu, Colloids Surf., A 245 (2004) 15–19.
[26] X. Liu, M.D. Kaminski, Y. Guan, H. Chen, H. Liu, A.J. Rosengart, J. Magn. Magn. Mater. 306 (2006) 248–253.
[27] T. Iwasaki, K. Kosaka, N. Mizutani, S. Watano, T. Yanagida, H. Tanaka, T. Kawai, Mater. Lett. 62 (2008) 4155–4157.
[28] M. Koneracká, P. Kopčanský, M. Timko, C.N. Ramchand, A. de Sequeira, M. Trevan, J. Mol. Catal. B: Enzym. 18 (2002) 13–18.
[29] R. Fernández-Pacheco, C. Marquina, J.G. Valdivia, M. Gutiérrez, M.S. Romero, R. Cornudellac, A. Labordad, A. Viloriad, T. Higuerad, A. Garcíad, J. Antonio García de Jalónd, M.R. Ibarraa, J. Magn. Magn. Mater. 311 (2007) 318–322.
[30] S. Wang, Y. Tan, D. Zhao, G. Liu, Biosens. Bioelectron. 23 (2008) 1781–1787.
[31] F. Sauzedde, A. Elaïssari, C. Pichot, Colloid Polym. Sci. 277 (1999) 846–855.
[32] L.N. Okassa, H. Marchais, L. Douziech-Eyrolles, S. Cohen-Jonathan, M. Soucé, P. Dubois, I. Chourpa, Int. J. Pharm. 302 (2005) 187–196.
[33] G.Y. Li, K.L. Huang, Y.R. Jiang, D.L. Yang, P. Ding, Int. J. Biol. Macromol. 42 (2008) 405–412.
[34] M.D. Torno, M.D. Kaminski, Y. Xie, R.E. Meyers, C.J. Mertz, X. Liu, W.D. O'Brien Jr., A.J. Rosengart, Thromb. Res. 121 (2008) 799–811.
[35] N.J. Darton, B. Hallmark, X. Han, S. Palit, N.K.H. Slater, M.R. Mackley, Nanomedicine 4 (2008) 19–29.
[36] N.A. Goldenberg, W.E. Hathaway, L. Jacobson, M.J. Manco-Johnson, Thromb. Res. 116 (2005) 345–356.
[37] J.C. Bacri, R. Perzynski, D. Salin, V. Cabuil, R. Massart, J. Magn. Magn. Mater. 85 (1990) 27–32.
[38] L. Packer, S. Tristram, J.M. Herz, C. Russell, C.L. Borders, FEBS Lett. 108 (1979) 243–248.
[39] A. Blinč, J. Magdic, J. Fric, I. Muševič, Fibrinolysis Proteol. 14 (2000) 288–299.
[40] N.K. Sarkar, Nature 185 (1960) 624–625.
[41] A.A. Smith, L.J. Jacobson, B.I. Miller, W.E. Hathaway, M.J. Manco-Johnson, Thromb. Res. 112 (2003) 329–337.
[42] T.D. Dziubla, V.V. Shuvaev, N.K. Hong, B.J. Hawkins, M. Madesh, H. Takano, E. Simone, M.T. Nakada, A. Fisher, S.M. Albelda, V.R. Muzykantov, Biomaterials 29 (2008) 215–227.